HTD-Vol. 183

HEAT TRANSFER ENHANCEMENT IN ELECTRONICS COOLING

presented at
THE WINTER ANNUAL MEETING OF
THE AMERICAN SOCIETY OF MECHANICAL ENGINEERS
ATLANTA, GEORGIA
DECEMBER 1–6, 1991

sponsored by
THE HEAT TRANSFER DIVISION, ASME

edited by
S. H. BHAVNANI
AUBURN UNIVERSITY

M. GREINER
UNIVERSITY OF NEVADA–RENO

THE AMERICAN SOCIETY OF MECHANICAL ENGINEERS
United Engineering Center • □ • □ • 345 East 47th Street • □ • □ • New York, N.Y. 10017

HTD-Vol. 183, Heat Transfer Enhancement
in Electronics Cooling
ASME 1991

EFFECT OF COMPONENT GEOMETRY AND LAYOUT ON FLOW DISTRIBUTION FOR SURFACE MOUNTED ELECTRONIC COMPONENTS: A SMOKE FLOW VISUALIZATION STUDY

Y. Wang and A. J. Ghajar
School of Mechanical and Aerospace Engineering
Oklahoma State University
Stillwater, Oklahoma

ABSTRACT

The objective of this study was to examine the effect of component dimension, component geometry, component orientation and circuit pack component placement (inline vs. staggered) on flow distribution on a circuit pack. The experiments were conducted in a horizontal rectangular wind tunnel using aluminum blocks to simulate various electronic components. The experiments were conducted for two different Reynolds numbers, 1500 and 3000, based on the channel hydraulic diameter. Smoke was used as the flow visualization vehicle. Still photographs were used to capture the flow visualization images. The experiments indicated that the component dimension (2-D vs. 3-D), orientation, geometry and location affects flow distribution over and around components and for populated circuit packs the staggered layout results in a better component flow exposure than the inline arrangement.

NOMENCLATURE

A_c	cross-sectional area
D^*	roughness ratio, t/H
D_H	hydraulic diameter, $4A_c/P$
H	channel height
L	component length along flow direction
P	perimeter
r	component radius
Re	Reynolds number based on hydraulic diameter, $D_H\overline{V}/\nu$
S	distance between two components along flow direction (groove)
SW	distance between two components normal to the flow direction
t	component height
V	local velocity
$\overline{V}$	mean velocity
V_{max}	maximum or center-line velocity
W	component width normal to the flow direction
y	normal spatial coordinate
ν	kinematic viscosity

INTRODUCTION

Technological advances have produced microminiaturized integrated circuits with very high electronic component densities and correspondingly large cooling heat flux requirements. Heat transfer thus has become an extremely important consideration in the design of the high speed digital electronics which are at the forefront of modern engineering and science research and development. The design of computer systems with acceptable reliability requires accurate predictions of component operating temperatures. Accurate prediction of component temperature depends on the heat transfer coefficient which in turn is influenced by the flow distribution over and around components, the placement of the components on a circuit pack and the size of the components.

Flow visualization studies over an array of electronic-like components using dye, smoke and oil-lampblack have been performed by several investigators (Azar and Russell, 1991; Garimella and Eibeck, 1990; Lehmann and Wirtz, 1985; Moffat et al., 1985; Sparrow et al., 1983). The results of these studies help in understanding of the influence of certain parameters on the flow distribution over electronic-like components. However, these studies either have had a limited scope or have been performed in water tunnels as opposed to wind tunnels. Since most electronic equipments use air as a cooling medium to reduce the temperature in the circuit packs, a wind tunnel was used to study the influence of flow and geometric parameters on the flow distribution over and around components.

The objective of this study was to examine the effect of component dimension, component geometry, component orientation and circuit pack component placement (inline vs. staggered) on flow distribution on a circuit pack. The experiments were conducted in a horizontal rectangular wind tunnel using aluminum blocks to simulate various electronic components. Smoke was used as the flow visualization vehicle. Still photographs were used to capture the flow visualization images.

EXPERIMENTAL SETUP AND PROCEDURES

A schematic diagram of the apparatus used in the experiments is shown in Fig. 1. The test component arrays were mounted along the top wall of a 1.52 m long rectangular duct with a fixed 25.4 cm width and a height that was easily adjustable from 1.27 to 7.62 cm. Ambient air was drawn past the components by a variable speed blower (New York Blower compact G. I. Fan, size 106 with 2 HP

and 3600 rpm motor) mounted downstream of the rectangular duct. Flow straighteners, a screen, and a large entrance contraction (contraction ratio varied from 14 to 42, depending on the channel height) provided a uniform, low turbulence flow at the entrance to the duct. The start of the test component array was positioned 0.76 m from the entrance to the duct and extend for 0.38 m downstream. The final 0.38 m of the duct was a constant area exit section. The duct emptied to an acoustically absorbent plenum (81 cm long, 76 cm wide and 28 cm high) that served to isolate the test flow from the blower noise. The air velocity was measured and adjusted (via a damper) in the round duct between the plenum and the blower by an MKS model 223 BD differential pressure transducer and a pitot static tube. The duct was traversed by the pitot static tube and the local velocities were then numerically integrated to render the mean velocity in the duct. The mean velocity of the air in the duct can vary from 0.1 to 15 m/s. The blower was mounted within an insulated box and exhausted outside the building, allowing flow visualization experiments with smoke to be performed. The rectangular duct is made of 1.27 cm thick plexiglas. To accommodate variation in the height of the duct, the setup was constructed such that the bottom part of the contraction with the entire duct floor can all be moved together and adjusted for the desired duct height. This design prevented flow disturbances caused by the sharp leading edges of splitters or adjustable flaps used by other investigators to adjust the duct height by moving the test section floor only. The test section is designed such that its upper wall can be removed and reset in place quickly, thus enabling rapid access to the array of components.

To verify flow uniformity in the test section, the velocity profiles just upstream and downstream of the component test section were measured with a pitot static tube and a differential pressure transducer. These measurements were made at three different locations across the width of the channel (at channel center line and about 1 cm from the wall on either side of the channel center line) and upto fifteen locations (depending on the channel height) across the height of the channel. Velocity profiles for different flow settings (low, medium and high velocities) at different locations indicated reproducible, uniform and symmetric velocity profiles. Figure 2 shows a typical velocity profile for the flow visualization experiments. The results presented in this figure are for a channel height of 7.62 cm and the velocity profiles were obtained at three different locations across the width of the channel just upstream and downstream of the component test section (76 cm and 114 cm from the entrance to the rectangular duct).

To visualize the flow distribution over and around components, smoke was used as the flow visualization vehicle. A schematic diagram of the smoke generator is shown in Fig. 3. CO_2 under pressure is fed in through a heated pipe into the heating chamber where it combines with a special light oil (velocite oil #10 purchased from Mobil Oil Company). The mixture is then heated in the heating chamber and the generated smoke is discharged through the discharge nozzle. The discharge nozzle is connected to the "smoke test plate" by a flexible hose. For the flow visualization experiments the removable upper wall of the test section was replaced with the smoke test plate. A schematic diagram of the smoke test plate is shown in Fig. 4. This device consisted of a wooden plate with the exact dimensions of the removable upper wall of the test section and a smoke chamber. The function of the smoke chamber is to distribute the smoke produced by the smoke generator into the flow field through a smoke slot (4 mm wide, 20.32 cm long) at the bottom of the smoke chamber. The electronic-like components made of aluminum blocks were placed on the smoke test plate.

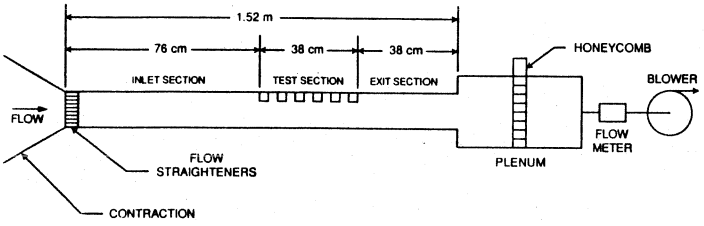

Figure 1. Schematic of the experimental apparatus.

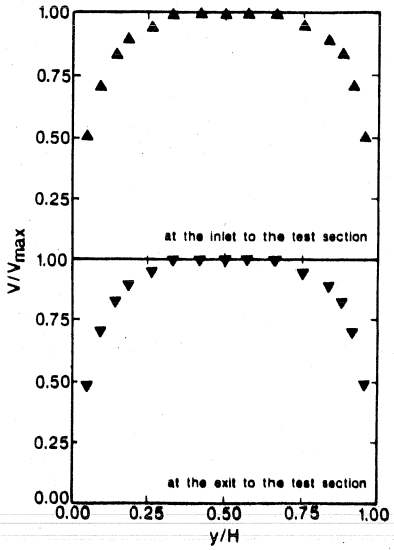

Figure 2. Dimensionless velocity profile at the inlet and exit of the component test section.

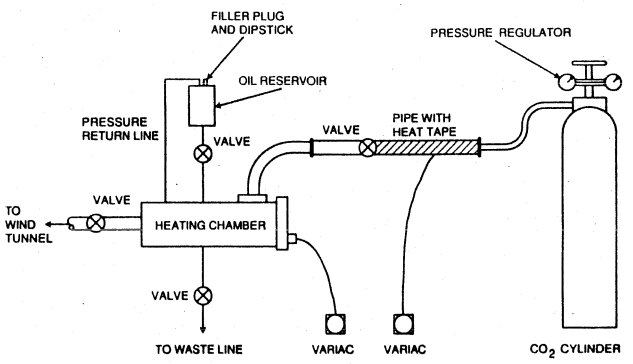

Figure 3. Schematic of the smoke generator.

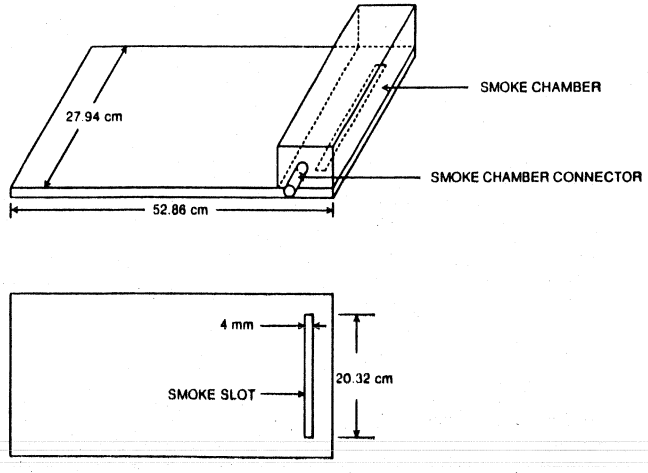

Figure 4. Schematic of the smoke test plate.

RESULTS AND DISCUSSION

The flow visualization experiments were conducted for a test section height of 7.62 cm and two different Reynolds numbers of 1500 and 3000, based on the channel hydraulic diameter. At 7.62 cm height of the test section, velocities of 0.2 and 0.4 m/s correspond to Reynolds numbers of 1500 and 3000, respectively.

Several parameters that could affect the flow distribution over and around components were studied such as, component dimension, component geometry, component orientation and circuit pack component placement (inline vs. staggered). The key dimensions describing the flow visualization experiments are (see Fig. 5):

- S = distance between two components along flow direction (groove)
- H = channel height
- L = component length along flow direction
- t = component height
- W = component width normal to the flow direction
- SW = distance between two components normal to the flow direction
- D* = t/H, the roughness ratio.

Still photographs were taken either at the side of the test section which will be referred to as side view photo or at the bottom of the test section (bottom view photo). Since the component test plate (smoke test plate) was placed on the top of the component test section, the components had to be also located on the top of the channel. Smoke came out from the top of the component test section in front of the components along flow direction (refer to Fig. 4). In order to eliminate the impact of the side walls, for most of the experiments, the components were put at the center of the channel and inline to the smoke source. Two face adhesive tape was employed to attach the components to the top plate of the wind tunnel. The specific parameters of each experiment are indicated below each photo (figure) presented next. It should be pointed out that the main objective of the flow visualization studies presented here were two fold: 1) to show the capability of our experimental setup by duplicating some of the flow visualization results of the other investigators and 2) to compliment the existing flow visualization studies.

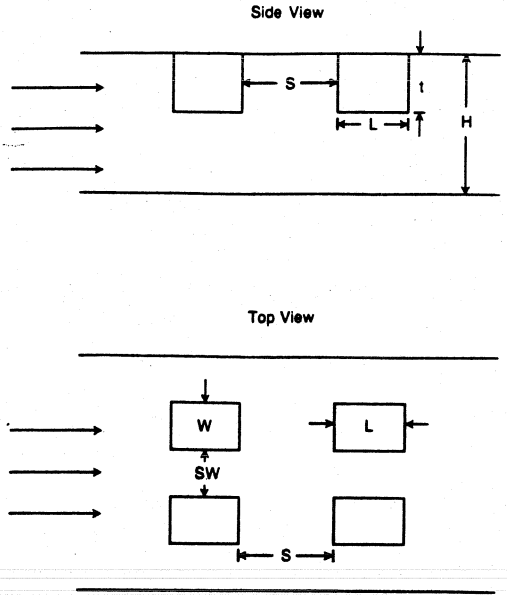

Figure 5. Nomenclature of the test conditions.

Component Dimension (2-D vs. 3-D)

A component is considered two-dimensional if its width occupies the entire cross-section of the channel. Figures 6-a and 6-b (2-D) and Figs. 6-c and 6-d (3-D) show the comparison between the two and three dimensional components. Figures 6-a through 6-d show that the flow patterns and distribution are very different for two and three dimensional components. Figures 6-a and 6-b show that most of the smoke trace passed the top of the component(s) with hardly any smoke being observed passing the sides of the component(s). However, Figs. 6-c and 6-d show much more activity on the side of the component(s). In addition, Fig. 6-d clearly shows more groove (S, distance between two components along flow direction) activity than the 2-D flow (see Fig. 6-b). Therefore, in the case of a heat dissipating component, there will be more interaction between the flow inside the groove (which is normally at a higher temperature than the main stream) and the main stream flow.

Component Geometry

The flow distribution inside the circuit packs will be affected by the shape of the component. Four configurations were used for investigating the impact of geometry on flow distribution. These were two square components with different layouts in the direction of the flow, a cylindrical and a rectangular component. All four experiments were conducted at D* = t/H = 0.33 and Reynolds number of 3000.

Figures 7-a through 7-d show the comparison of the flow patterns for the different configurations. For the component with the smallest t/W value (Fig. 7-a), the stagnation point, location where flow velocity reaches zero in the direction of the flow (white color point in the figures before the component along the flow direction), is far away from the component edge and the flow (smoke) distribution around the component is large. Comparison of Figs. 7-a (with the smallest t/W) and 7-b (with the largest t/W) clearly shows this affect. For the component in Fig. 7-c with a t/W = 0.67, the flow distribution around the component is about three times as wide as the component width W (diameter). The stagnation point in this case is closer to the component edge than the component shown in Fig. 7-a with a t/W = 0.5. Comparison of Figs. 7-b and 7-d indicates that the component with multiple angles (at least more than two faces facing the flow direction, Fig. 7-d) even though the t/W value is slightly smaller than the rectangular component shown in Fig. 7-b (only one surface faces the streamwise direction), the stagnation point is closer to component edge, as shown in Fig. 7-d. Generally speaking, better flow exposure will be exhibited with larger t/W ratios which leads to a smaller flow distribution around the component. With the same t/W value, a round component has a better flow distribution than a multiple angle component and a multiple angle component has a better flow distribution than a rectangular component.

Component Orientation

The effect of component orientation on flow distribution around the component is shown in Figs. 7-a, 7-d and 8 for Re = 3000 and D* = 0.33. As mentioned earlier, the ratio of t/W is significant on the flow distribution around the component. By comparison of these figures, it can be concluded that the orientation with higher t/W ratio (Fig. 8) leads to a significant decrease in the flow distribution around the component than those shown in Figs. 7-a and 7-d with lower t/W ratios. Therefore, placing components with their longest side parallel to the direction of the flow will reduce mixing and may enhance component flow exposure.

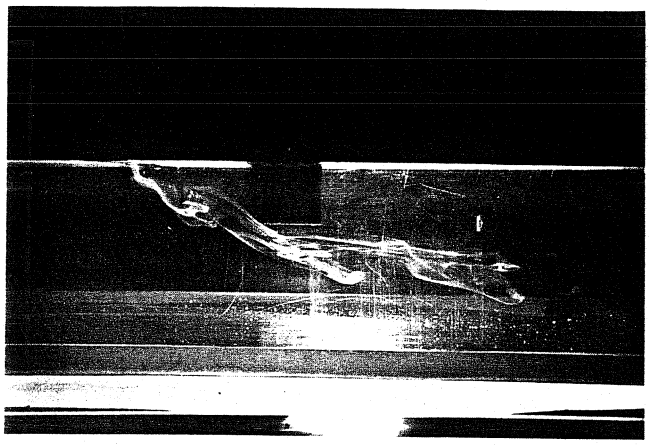

Figure 6-a. Side view of flow over one 2-D component (Re = 1500, D* = 0.33, t = L = 2.54 cm, W = 25.4 cm).

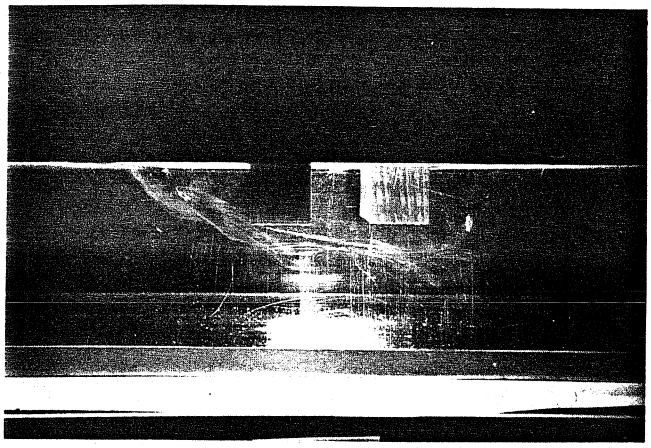

Figure 6-b. Side view of flow over two 2-D components (Re = 1500, D* = 0.33, t = L = S = 2.54 cm, W = 25.4 cm).

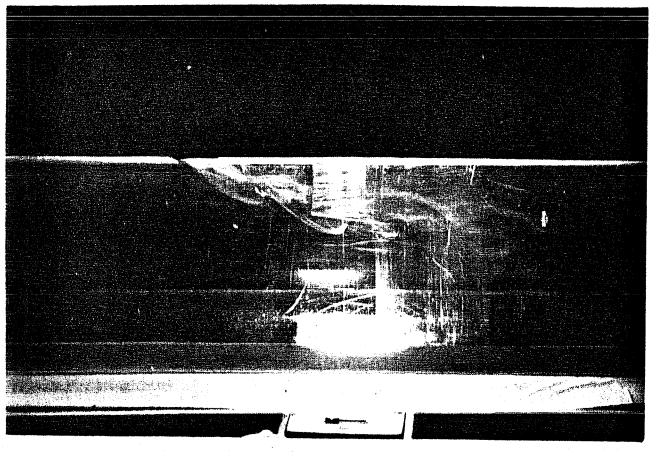

Figure 6-c. Side view of flow over one 3-D component (Re = 1500, D* = 0.33, t = L = 2.54 cm, W = 3.13 cm).

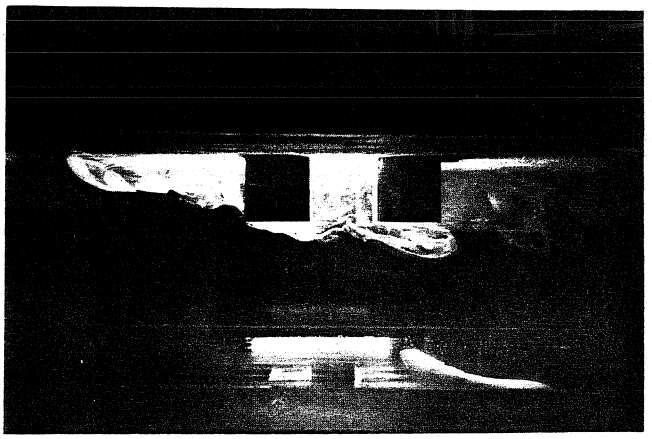

Figure 6-d. Side view of flow over two 3-D components (Re = 3000, D* = 0.33, t = L = S = 2.54 cm, W = 3.13 cm).

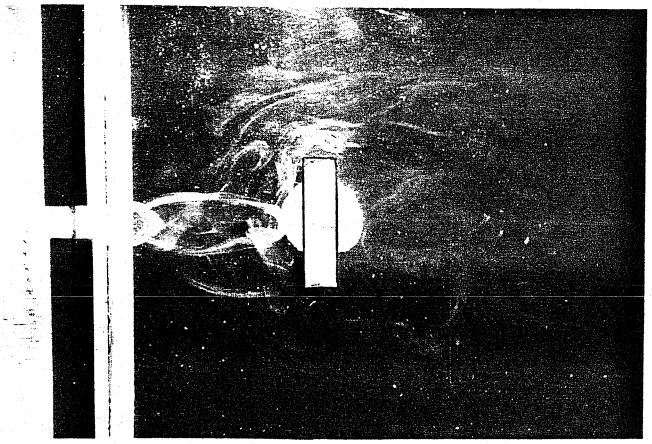

Figure 7-a. Bottom view of flow over a rectangular component (Re = 3000, D* = 0.33, W = 5.08 cm, t = 2.54 cm, L = 1.27 cm, t/W = 0.5).

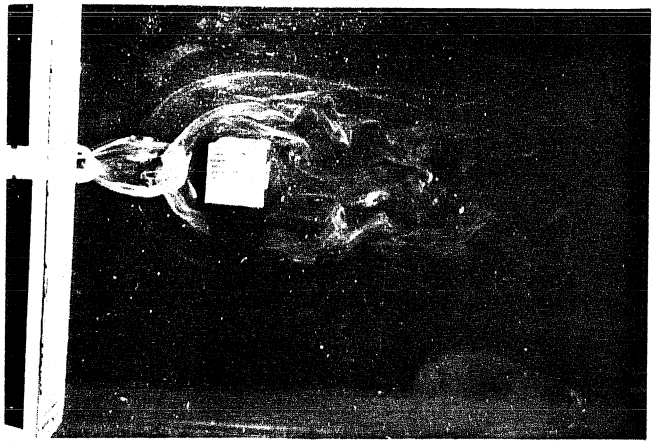

Figure 7-b. Bottom view of flow over a rectangular component (Re = 3000, D* = 0.33, t = W = L = 2.54 cm, t/W = 1).

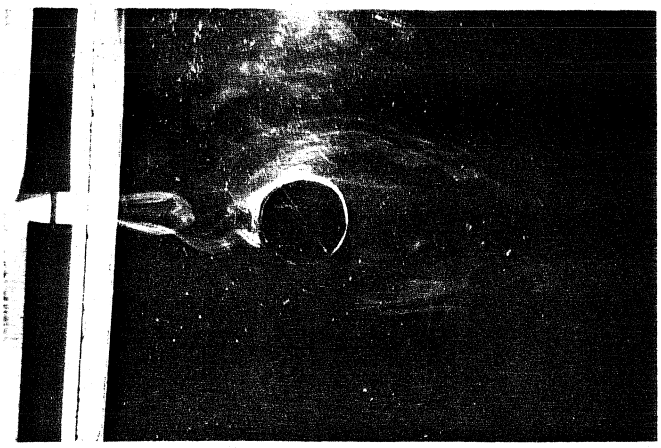

Figure 7-c. Bottom view of flow over a round component (Re = 3000, D* = 0.33, r = 1.91 cm, t = 2.54 cm, t/W = 0.67).

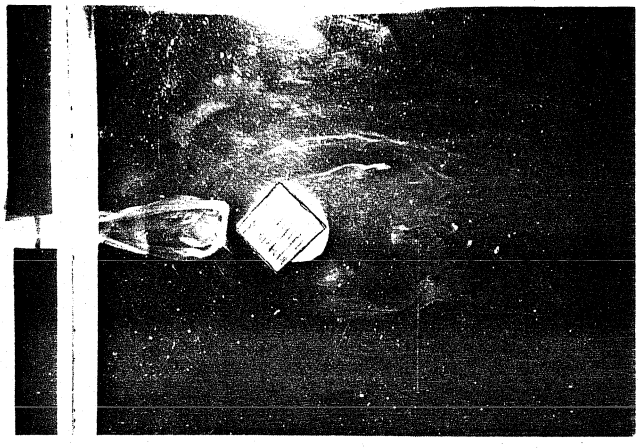

Figure 7-d. Bottom view of flow over a multiple angle component (Re = 3000, D* = 0.33, t = L = 2.54 cm, W = 3.59 cm, t/W = 0.707).

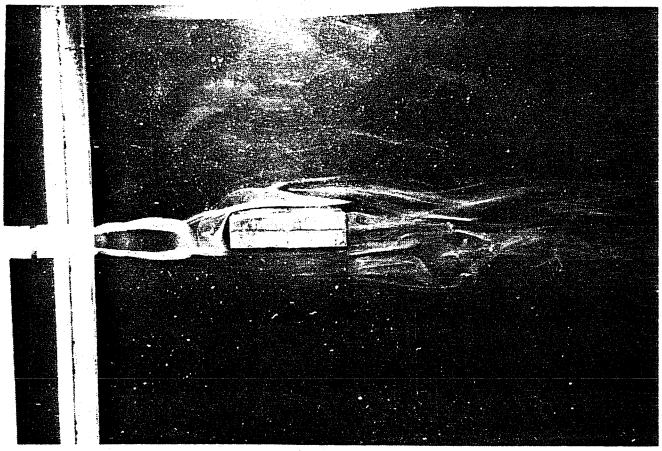

Figure 8. Bottom view of flow over one component (Re = 3000, D* = 0.33, L = 5.08 cm, W = 1.27 cm, t = 2.54 cm, t/W = 2).

Circuit Pack Component Placement

The flow visualization results discussed in this section have a Reynolds number of 3000 and a staggered or inline arrangement.

(1) Figures 9-a and 9-b show that for the staggered layout, components demonstrate more flow exposure than the inline arrangement because the grooves communicate with the mainstream directly.

(2) Increasing S (the space between components in the flow direction) will gain more flow exposure for the components and vice versa, see Figs. 10-a through 10-d. The figures also show that with the same square component size reducing S will decrease the flow exposure significantly than reducing SW (the space between components perpendicular to the flow direction) especially for inline layout, see Figs. 10-b and 10-d.

(3) Figures 11-a and 11-b show that placing the taller component at the first row or the mid row, will generate large areas of stagnation in the fore and aft of the components. This reduces the flow interactivity. By allocating the taller components to the last row, the stagnation areas are no longer present, see Fig. 11-c. Therefore, taller components or components with large aspect ratio should be placed at the outlet of the circuit pack channel.

SUMMARY AND CONCLUSIONS

The smoke flow visualization results presented in this study support the general conclusions reached by other investigators. The important specific conclusions of this study are:

1. Component Dimension - Flow patterns and distribution are very different for two and three dimensional components.

2. Component Geometry - Components with smaller t/W ratio will have less flow exposure in the wind tunnel. The flow exposure varies with t/W, component geometry and Reynolds number. With the same t/W ratio, a round component has a better flow distribution (exposure) than a multiple angle component and a multiple angle component has a better flow distribution than a single face component.

3. Component Orientation - Placing a component such that the longest side of the component is parallel to the flow will lead to better flow distribution. Hence, component orientation will effect flow distribution directly.

4. Circuit Pack Component Placement (populated circuit packs) - (a) Staggered layout results in a better flow exposure than inline arrangement. (b) Increasing S will gain more flow exposure and vice versa. With the same square component size, reducing S will decrease the flow exposure significantly than reducing SW, especially for inline layout. (c) Tall components or components with large aspect ratio should be placed at the outlet of the circuit pack.

ACKNOWLEDGMENT

The wind tunnel used in this study for flow visualization experiments was designed and constructed by Mr. M. Arabzadeh, a Ph.D. candidate.

Figure 9-a. Bottom view of flow through a staggered circuit pack, ten components (Re = 3000, D* = 0.33, L = S = t = W = SW = 2.54 cm).

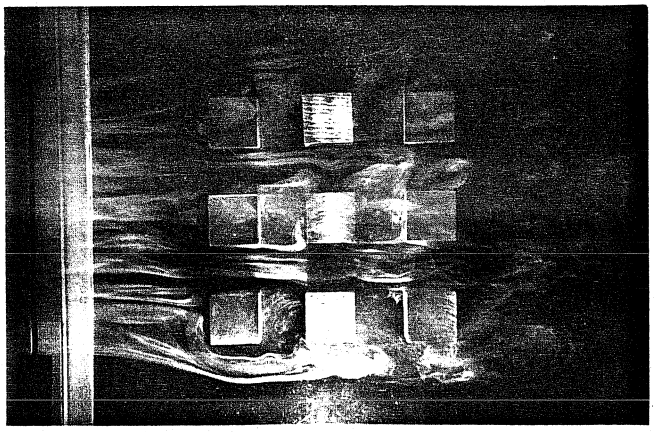

Figure 9-b. Bottom view of flow through an inline circuit pack, nine components (Re = 3000, D* = 0.33, L = S = t = SW = 2.54 cm).

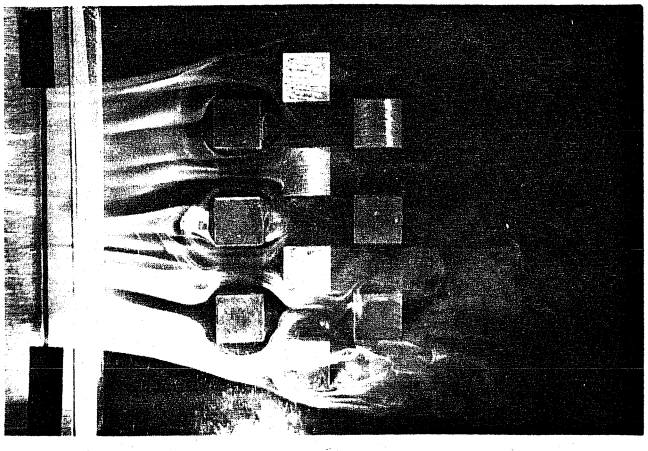

Figure 10-a. Bottom view of flow through a staggered circuit pack, ten components (Re = 3000, D* = 0.33, S = 1.27 cm, L = W = t = SW = 2.54 cm).

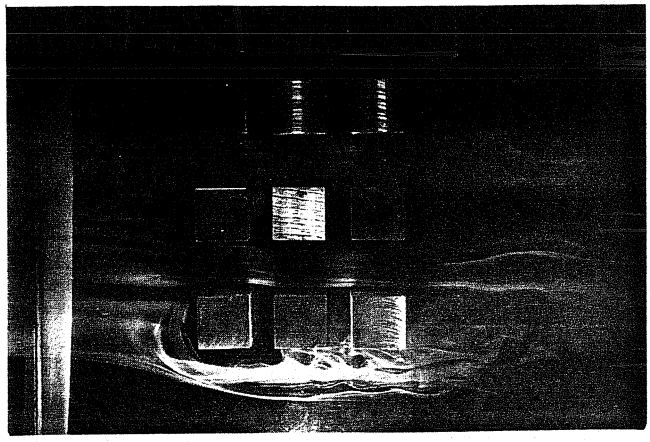

Figure 10-b. Bottom view of flow through an inline circuit pack, nine components (Re = 3000, D* = 0.33, S = 1.27 cm, L = W = t = SW = 2.54 cm).

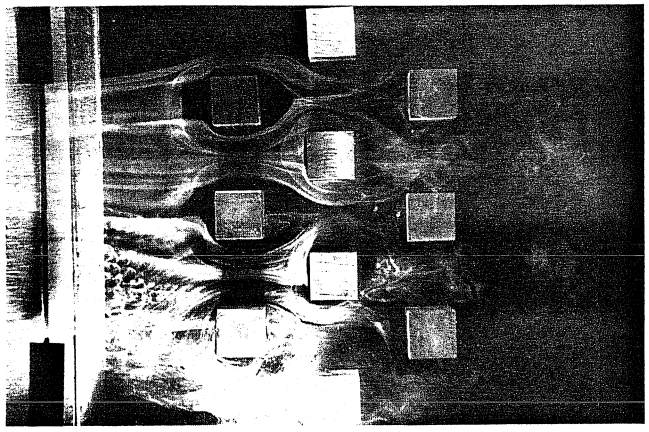

Figure 10-c. Bottom view of flow through a staggered circuit pack, ten components (Re = 3000, D* = 0.33, SW = 3.81 cm, L = W = S = t = 2.54 cm).

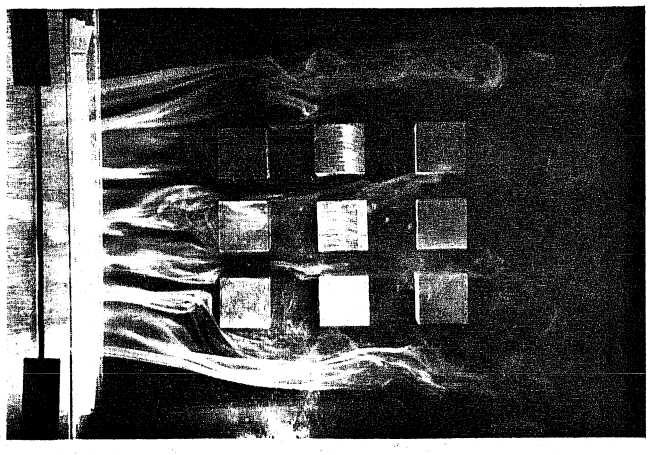

Figure 10-d. Bottom view of flow through an inline circuit pack, nine components (Re = 3000,D* = 0.33, SW = 1.27 cm, L = W = S = t = 2.54 cm).

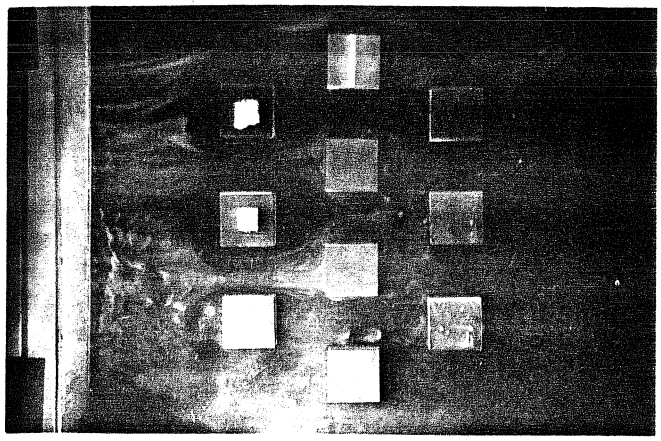

Figure 11-a. Bottom view of flow through a staggered circuit pack, taller components marked with tape are placed in the first row (Re = 3000, L = W = S = SW = 2.54 cm, t_{tall} = 2.54 cm, t_{short} = 1.27 cm).

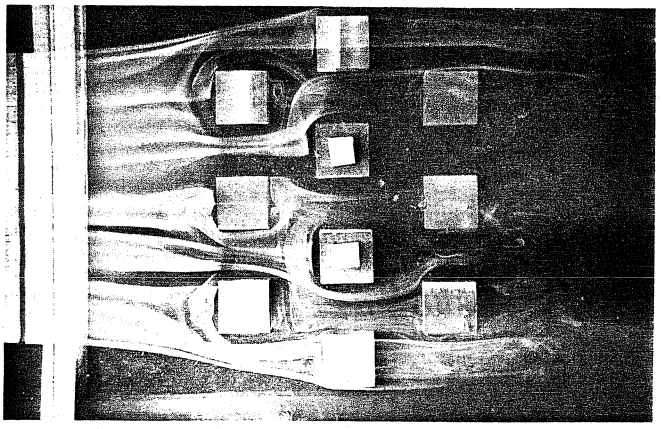

Figure 11-b. Bottom view of flow through a staggered circuit pack, taller components marked with tape are placed in the second row (Re = 3000, L = W = S = SW = 2.54 cm, t_{tall} = 2.54 cm, t_{short} = 1.27 cm).

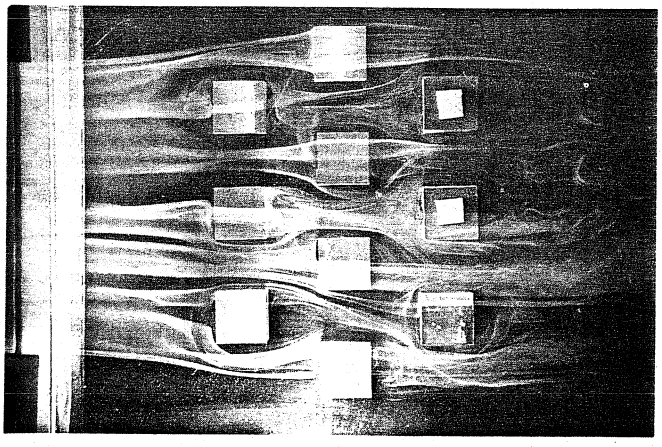

Figure 11-c. Bottom view of flow through a staggered circuit pack, taller components marked with tape are placed in the third row (Re = 3000, L = W = S = SW = 2.54 cm, t_{tall} = 2.54 cm, t_{short} = 1.27 cm).

REFERENCES

Azar, K. and Russell, E. T., 1991, "Effect of Component Layout and Geometry on the Flow Distribution in Electronic Circuit Packs," Journal of Electronic Packaging, Vol. 113, 50-57.

Garimella, S. V. and Eibeck, P. A., 1990, "Onset of Transition in the Flow Over a Three-Dimensional Array of Rectangular Obstacles," Thermal Modeling and Design of Electronic Systems and Devices, ASME HTD-Vol. 153, 1-6.

Lehmann, G. L. and Wirtz, R. A., 1985, "The Effect of Variations in Stream-Wise Spacing and Length on Convection From Surface Mounted Rectangular Components," Heat Transfer in Electronic Equipment-1985, ASME HTD-Vol. 48, 39-47.

Moffat, R. J., Arvizu, D. E. and Ortega, A., 1985, "Cooling Electronic Components: Forced Convection Experiments in an Air-Cooled Array," Heat Transfer in Electronic Equipment-1985, ASME HTD-Vol. 48, 17-27.

Sparrow, E. M., Vemuri, S. B. and Kadle, D. S., 1983, "Enhanced and Local Heat Transfer, Pressure Drop, and Flow Visualization for Arrays of Block-Like Electronic Components," Int. J. Heat Mass Transfer, Vol. 26, No. 5, 689-699.